J Neurooncol (2011) 101:419–428
DOI 10.1007/s11060-010-0275-9

LABORATORY INVESTIGATION - HUMAN/ANIMAL TISSUE

Variable methylation of the imprinted gene, SNRPN, supports a relationship between intracranial germ cell tumours and neural stem cells

Shih-Han Lee · Vanessa Appleby · Jennie N. Jeyapalan · Roger D. Palmer · James C. Nicholson · Virginie Sottile · Erning Gao · Nicholas Coleman · Paul J. Scotting

Received: 4 February 2010 / Accepted: 16 June 2010 / Published online: 26 June 2010

Abstract Germ cell tumours (GCTs) are a diverse group of neoplasms all of which are generally believed to arise from germ cell progenitors (PGCs). Even those that form in the nervous system are likewise believed to be PGC-derived, despite being found a great distance from the normal location of germ cells. The primary evidence in favour of this model for the origins of intracranial GCTs is that they share molecular features with other GCTs. Those features include shared gene expression and a lack of methylation of imprinted genes, including SNRPN. Contrary to this model, we have proposed that endogenous neural stem cells of the brain are a more likely origin for these tumours. We show here that the lack of methylation of SNRPN that has previously been taken to indicate an origin for GCTs from PGCs is also seen in neural stem cells of mice and humans. We believe that, in the light of these and other recent observations, endogenous neural precursors of the brain are a more plausible origin for intracranial GCTs than are misplaced PGCs.

Keywords Intracranial · Germ cell tumour · Germinoma · SNRPN · Imprinting

S.-H. Lee · V. Appleby · J. N. Jeyapalan · E. Gao · P. J. Scotting (✉)
Children's Brain Tumour Research Centre, Institute of Genetics, University of Nottingham, Queen's Medical Centre, Nottingham NG7 2UH, UK
e-mail: paul.scotting@nottingham.ac.uk

V. Sottile
Wolfson Centre for Stem Cells, Tissue, Engineering and Modelling (STEM), School of Clinical Sciences, The University of Nottingham, Nottingham NG7 2RD, UK

R. D. Palmer · N. Coleman
MRC Cancer Cell Unit, Hutchison/MRC Research Centre, Box 197, Hills Road, Cambridge CB2 0XZ, UK

R. D. Palmer · J. C. Nicholson
Department of Paediatric Oncology, Addenbrooke's Hospital, Box 181, Hills Road, Cambridge CB2 0QQ, UK

Introduction

Germ cell tumours (GCTs) are grouped together on the basis that they originate from germ cell progenitors (PGCs). They are found in both gonadal and non-gonadal locations and exhibit diverse tumour phenotypes [1]. These include relatively homogeneous cell populations (germinomatous), presumed to be closely related to the PGC progenitor, and those made up of a wide range of tissues, either with a large extraembryonic component (Yolk sac tumours (YSTs) and choriocarcinomas) or predominantly embryonic tissue (embryonal carcinomas, also referred to as teratocarcinomas), reflecting the broad developmental potential of the progenitor cell. Clinically, these tumours vary enormously in their outcomes. Treatment often includes radiotherapy with associated morbidity including endocrine and neuropsychological deficits [2].

Although most GCTs occur in the gonads, GCTs in the young are predominantly extra-gonadal [1]. The occurrence of these tumours is restricted to specific times and locations. In older children and in adults, extragonadal GCTs are most commonly found in the brain and less frequently in the mediastinal region. Within the brain, GCTs diagnosed perinatally are most often teratomas and, despite a benign biology, are almost invariably fatal due to their size and their impact upon normal brain development. Most other intracranial GCTs are diagnosed around the time of puberty, when about 60% are germinomas and

about 40% are non-germinomas or of mixed geminomatous/YST histology. Intracranial GCTs develop almost exclusively in the ventral midline of the brain, with a bias towards the pineal region in boys and the suprasellar region (near to the hypothalamus) in girls. The generally accepted explanation for these restricted sites in which germinomas occur is that they reflect the midline migration route of PGCs during early embryonic development. The underlying theory is that 'rogue' PGCs become mis-located during their embryonic migration. These mis-placed cells then avoid the normal apoptotic fate of PGCs outside the gonads during early embryogenesis to become apparent only later when their tumorigenic potential is realized, an argument that appears less applicable to the tumours of infants and neonates. Hence, extragonadal GCTs are almost unique amongst cancers, in that they are believed to arise at sites distant from the normal location of their progenitor cell.

Although it has been traditionally accepted that all GCTs arise from PGCs, a number of anomalies have led to some dissent from this view. One major concern is that PGCs do not travel through or near the locations of most extragonadal GCTs, and indeed migrate very little during embryonic development [3]. Their apparent migration can be accounted for largely by changes in the relative spatial orientations of the tissues that carry them [3]. It is therefore unclear why such cells would become mis-located at a site as distant as the brain. Indeed, Runyan et al. [4] studied extragonadal PGCs in Bax null mice, which leads to a disruption of the apoptosis through which misplaced PGCs would normally be eliminated. They found that many PGCs survived outside of the gonads in these Bax null mice, but none were found in the brain. This led them to comment that, although there were other explanations, 'we cannot exclude the possibility that human EGCTs in those locations don't come from germ cells at all, but are derived from other stem cell populations'.

The central line of argument linking intracranial GCTs to a PGC origin is that they share features in common with PGCs, or at least other GCTs, that are not exhibited by any potential progenitor cell endogenous to the brain itself. One of the main features that provide this link to PGCs is the shared methylation status of imprinted genes between intracranial GCTs and GCTs from other locations, including the gonads. However, even this does not provide a definitive link.

Amongst the normal cells of the body, PGCs are unusual because, unlike somatic cells where either the maternal or paternal copy of imprinted genes are irreversibly methylated, this methylation is briefly erased during the migratory phase of PGC development. Thus, tumours that arise from immature PGCs might develop without this methylation being re-established. Such a lack of methylation is seen in a large proportion of gonadal and non-gonadal GCTs [5, 6]. However, lack of methylation of one such locus, IGF-2, and some other imprinted genes is also seen in several non-GCT classes of tumour [7–12]. The only imprinted gene where lack of complete methylation is restricted to GCTs and PGCs is SNRPN. However, even in the case of SNRPN, Bussey et al. [13] found that only a minority of extragonadal GCTs exhibited a non-somatic, PGC-like pattern of methylation of the SNRPN gene.

The evidence in favour of alternative origins for some GCTs has been reviewed by Oosterhuis [14] and Scotting [15]. However, the absence of methylation of SNRPN in some extragonadal GCTs has remained one of the strongest links used to argue in favour of a PGC origin for these tumours. In this paper we show that this feature of GCTs is in fact also shared with the endogenous Neural Stem Cells (NSCs) of the brain. Our detailed analysis of SNRPN methylation in a cohort of GCTs also shows that they are hypomethylated but they do not show complete absence of methylation. Given their abundance in the very tissue where these tumours form, NSCs should therefore now be considered as strong candidates for the origin of these tumours.

Materials and methods

Mouse neural stem cell culture

Tissue samples were dissected and homogenized in ice cold PBS. Depending on the amount of tissue, 2–5 ml of Accumax (PatriCell) was used to dissociate the cells. After washing with PBS, cell pellets were resuspended in complete culture medium [Neurobasal and DMEM F12 (Gibco) equally mixed medium supplemented with Penicillin/Streptomycin (Sigma), B27 and N2 (Gibco), 20 ng/ml growth factors (FGF and EGF, Invitrogen)] and seeded into culture wells. All cells were incubated at 37°C in a 5% CO_2 humidified incubator. To passage cells, Accutase (PatriCell) was utilized to dissociate the spheres into single cells. These cells were established as NSCs by their ability to be propagated over multiple passaging as neurospheres and the ability to differentiate into both neuronal and glial lineages (data not ahown).

Human neural stem cell line culture

Following the manufacturer's instructions, the human ReNcell VM NSC line (Millipore Corp., Bedford, MA, U.S.A) was maintained as adherent cells in laminin-coated flasks (final concentration of 15 μg/ml, Sigma Cat. No. L-2020) with ReNcell NSC Maintenance Medium (Chemicon) supplemented with 20 ng/ml growth factors (basic fibroblast growth factor and epidermal growth factor,

Invitrogen) and maintained as suspended spheres in Neurobasal and DMEM F12 (Gibco) mixed medium supplemented with Penicillin/Streptomycin (Sigma), B27 and N2 (Gibco), 20 ng/ml growth factors (Invitrogen).

Genomic DNA purification and sodium bisulfite treatment

Cells and tissues were lysed in lysis buffer (0.1 M Tris, pH 8.5, 50 mM EDTA, 0.2 M NaCl, 0.2% SDS, 100 ng/μl ProteinaseK), and genomic DNA was precipitated by addition of an equal volume of isopropanol, washed by 70% ethanol, and dissolved in water. Banked frozen tissue was provided by the Children's Cancer and Leukaemia Group (CCLG; Biological Study 2002–03) from patients managed on UK paediatric treatment schedules. All specimens examined in the study initially underwent frozen section analysis, with independent review by three separate histopathologists. In the histopathological nomenclature used, germinoma refers to all tumours with germinomatous histology, regardless of site (i.e. testicular seminoma, ovarian dysgerminoma and extragonadal germinoma). Sections of tumours were homogenised (PolyTron PT2100) in TRIzol (Invitrogen, Paisley, UK) to preserve nucleic acids. Following the addition of chloroform, DNA was extracted from the interphase/organic phase using ethanol precipitation. The resultant DNA pellets were serially washed with 0.1 M sodium citrate in 10% ethanol, before resuspension in water (pH 8.4).

Genomic DNA of GCTs was acquired from the Children's Cancer and Leukaemia Group (CCLG) Biological Study 2002–03 (Cambridge UK). Human control somatic cell DNAs was obtained from (Promega) and from normal male adults (buccal cells). 1–2 μg of DNA from each sample was subjected to sodium bisulfite treatment using the EZ DNA Methylation Kit (Zymo Research, Orange County, CA USA) following the manufacturer's instructions.

Genescan anaylsis of *SNRPN*

The DMR1 region of *SnrpN* was amplified from sodium bisulfite-treated genomic DNA using FAM-labeled primers (MWG, Germany). Primer sequences for mouse samples were as described by Li et al. [16]: mSNRPN-DMR1F: 5′-TAT GTA ATA TGA TAT AGT TTA GAA ATT AG-3′; mSNRPN-DMR1R: 5′-AAT AAA CCC AAA TCT AAA ATA TTT TAA TC-3′. Sequences of primers for human samples were as described by Rugg-Gunn et al. [17] : PhuSNRPNBSF: 5′-GGT TTT TTT TTA TTG TAA TAG TGT TGT GGG G-3′; huSNRPN-BSR: 5′-CTC CAA AAC AAA AAA CTT TAA AAC CCA AAT TC-3′. 400 ng of each PCR product was digested using the HhaI enzyme at 37°C for at least 4 h. The digested products were separated by agarose gel electrophoresis and then examined by the Perkin-Elmer ABI Prism 3130 fluorescent DNA analyser. The data were analysed by the Peak Scanner Software v1.0 from ABI.

Bisulfite sequencing

Each PCR mixture contained 0.5 μmol primers, 0.75 mM dNTP (Invitrogen), 2 μl 10× buffer (Invitrogen), 1.5 mM $MgCl_2$, 50–100 ng template DNA, 0.75 unit Platinum Taq Polymerase (Invitrogen) and H_2O up to 20 μl. The PCR conditions and primer sequences were the same as described for Genescan analysis. PCR products were cloned into a TA vectors (either pGEM-T vector, Promega; pCR^RII vector, Invitrogen) and plasmid DNAs were sequenced.

Pyrosequencing

Our pyrosequencing analysis procedures were based on White et al. [18] with slight modification. Briefly, the bisulfite specific PCR reactions were performed with biotin-labeled primers (MWG, Germany) and sodium bisulfite treated genomic DNAs. The PCR mixture and condition were the same as those of bisulfite sequencing. DNA purification followed by sequencing (using Pyromark MD system) was carried out by the Scientific Support Services in the Wolfson Institute for Biomedical Research at the University of London (London, UK). PCR and sequencing primers were as described previously [18].

Results

Neural stem cells of the developing mouse brain exhibit variable methylation of SnrpN

Of all the features of intracranial GCTs, lack of methylation of SNRPN is the most specific to this class of tumour and one of the strongest lines of evidence in support of a PGC origin (Reviewed in [15]). We therefore set out to determine whether, as the literature suggests, lack of methylation of the SNRPN gene is unique to PGCs and GCTs. In particular, we asked whether populations of cells exist in the developing brain that also exhibit some lack of methylation of the maternal allele of SNRPN. In order to address this, we studied various stages of brain development in the mouse. The analysis so far carried out in human tumours used methylation-sensitive restriction sites and so tested the methylation status of 4 CpG dinucleotides within the regulatory region of the SNRPN gene [5]. Because there are two very close HhaI sites in the human gene, PCR products would be similarly digested if either of these sites

were not methylated. The detailed sequence in these non-coding regions is not tightly conserved between humans and mice, so we could not determine the methylation status of precisely the same CpG dinucleotides in mice using this same approach. However, two CpGs did again give rise to such a site in the Differentially Methylated Region 1 (DMR1) region, which has been shown to be the prime imprinting control region of the mouse SnrpN gene, and so we were able to carry out analysis analogous to that done in the human gene. As in the human gene, these CpGs constitute a recognition site for digestion with the 4 base cutter restriction enzyme, Hha1. We therefore used this enzyme to analyse the methylation status of the mouse gene.

Genomic DNA from different region of mouse brain tissue was treated with sodium bisulfite, converting unmethylated cytosines to uracil, thus removing the Hha1 sites (CGCG), where they were unmethylated. Following Hha1 digestion, we were therefore able to establish the proportion of alleles in which the Hha1 sites were protected by methylation. The expected ratio would be 50:50 for any somatic cell, with all maternal alleles protected. Any ratio of protected alleles less than this would indicate a proportion of maternal alleles that lacked methylation.

We first established that the conditions we used ensured that the restriction digestion would be complete. This demonstrated that complete digestion of a cloned SnrpN DMR1 region was achieved within 2 h (Fig. 1a). We next performed this analysis on dissected regions of brain from postnatal mouse brain. This analysis showed no sign, by visual inspection or densitometry analysis, of a pattern different to the expected somatic methylation, with approximately equal amounts of the band of 532 bp (representing unmethylated DNA) and the digested bands of 349 bp and 183 bp (representing methylated DNA) (Fig. 1b). However, these samples are composed largely of post-mitotic cells. Since we reasoned that any potential cell of origin of tumours was likely to be a proliferating progenitor cell in the ventral midline (VML) region where these tumours normally arise, we isolated NSCs from the VML of postnatal or embryonic mice to determine if these exhibited incomplete imprinting, which might not been seen in a background of more mature cells where imprinting was complete (Fig. 1c). In order to gain a more accurate quantitation of the results, we subjected these samples to Genescan analysis. FAM-labeled primers were used to prepare PCR products for HhaI digestion and Genescan analysis was used to measure the intensity of the digested and undigested products. NSCs showed a level of methylation similar to liver cells that were included as a somatically imprinted control (not shown). Again we verified that these digests had gone to completion by carrying out a time course digestion on one sample (Fig. 1d), showing that the final digestion pattern was

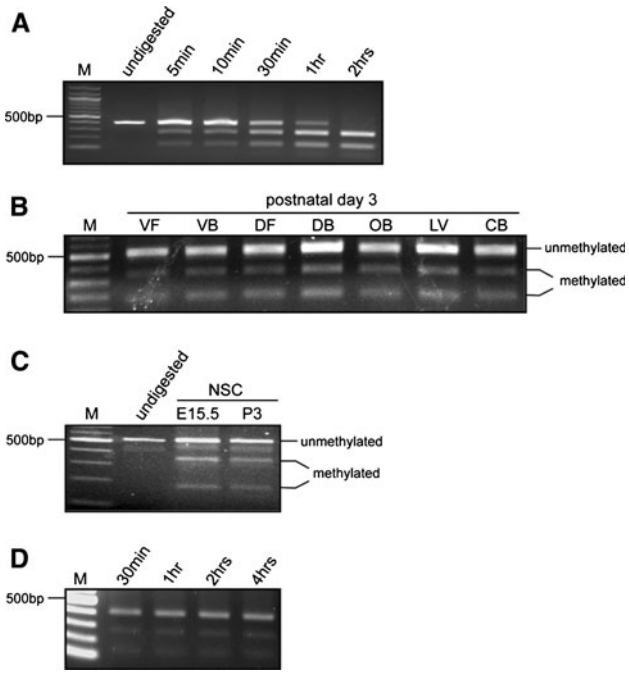

Fig. 1 Restriction digestion analysis of *SnrpN* methylation in developing mouse brain**. a** Time course of HhaI digestion. PCR products amplified from bisulfite-treated DNA was digested with HhaI for various times. This demonstrated rapid digestion to completion within 2 h for a control PCR product containing the target site. **b** HhaI digestion results demonstrating *SnrpN* methylation status in postnatal day 3 (P3) mouse brain. CB—cerebellum, DB—dorsal back, DF—dorsal front, LV—lateral ventricle, OB—olfactory bulb, VB—ventral back, VF—ventral front. **c** HhaI digestion results demonstrating *SnrpN* methylation status in E15.5 NSCs and P3 NSCs. **d** After 1h PCR products from NSCs reached a level of digestion that did not alter over time, demonstrating that this was complete digestion of all sequences containing the target site for HhaI

reached within 1 h of incubation, while all experimental digest were left for at least 3.5 h. It therefore seems that in these NSCs, there is no net difference in the methylation at these specific CpGs, from that seen in control somatic tissues.

We envisaged three possible explanations for this. Either, there is no variation in the methylation in mouse brain tissues or NSCs, or there is variation but the net result at these particular CpGs is neutral (equal levels of gains of methylation in paternal alleles and loss of methylation in maternal alleles) or there is variation in methylation of the DMR1 region of SnrpN, but these particular CpGs are not representative of the whole region. We therefore used bisulfite sequencing to determine the methylation status of CpGs across the entire DMR1 region that has been shown to be the prime imprinting control region of the mouse SnrpN gene.

Following sodium bisulfite treatment, the DMR1 region was PCR amplified, cloned and sequenced. While the DMR1 region was either entirely methylated or unmethylated (presumed to reflect the maternal and paternal alleles

respectively) in samples from the lateral ventricle and cortex, we saw some variation in the pattern of methylation in tissue from the VML (Fig. 2a), the region where germinomas arise in humans and also the region where IGF2 has been shown to be biallelically expressed in mice [19]. We next analysed DNA from NSCs isolated from the VML of embryonic or postnatal mice to determine if these exhibited incomplete methylation, and might therefore explain the low level of incomplete methylation seen in the tissue as described above. Our analyses showed that NSCs from the postnatal VML showed the pattern expected for somatic tissues, but there was a remarkable variation in imprinting in those isolated at E15.5 (Fig. 2b) with 11 of the 16 CpGs showing a methylation state inconsistent with the majority of the region's CpGs in some clones. However, this was sometimes absence of methylation where most CpGs were methylated and sometimes methylation in a background of general non-methylation. It was notable that the methylation status of at least one of the CpGs that represented the Hha1 sites always matched the general methylation of the region as a whole. It is not, therefore, surprising that the Hha1 analysis failed to detect this variation that was revealed by bisulfite sequence analysis.

Together, these results show that some NSCs from restricted locations in the developing mouse brain, especially cells from the VML at prenatal stages, exhibit a more 'relaxed' methylation status than expected for somatic cells. This pattern is quite similar to that seen in PGCs as they reset their methylation during embryonic development [16, 20].

Human NSCs exhibit variable methylation of SNRPN

The above data suggest that the methylation status of the SnrpN gene is variable in progenitor cells of the developing mouse brain. This provides grounds to suspect that human NSCs might also exhibit a pattern of methylation different to other somatic cells. In order to analyse this we made use of the ReNcell® VM Neural Stem Cell Line (Millipore). This stable human cell line is derived from the ventral mesencephalon region of human fetal brain (ten-week gestation fetal midbrain tissue) and shows all the features of NSCs; these cells can self-renew, proliferate and, under appropriate culture conditions, differentiate into both glial and neuronal cell types [21].

Since the SNRPN gene in these human cells should share an almost identical sequence to the gene studied in GCTs by Schneider et al. [5] and Bussey et al. [13] we were able to carry out the same analysis that they used to study SNRPN methylation. Genomic DNA from these cells was treated with sodium bisulfite and PCR products subjected to Hha1 digestion. We used the same approach of restriction enzyme sensitivity to determine the ratio of cut to uncut DNA (Fig. 3). Comparing the ReNcell NSC value to that for somatic controls, ReNcell NSCs appeared hypomethylated. We quantified this in two ways. First we compared the result for NSCs with various ratios of clones known to be entirely methylated or unmethylated, which showed that the NSCs appeared to have a unmethylated/methylated ratio of between 70/30 and 80/20 (Fig. 4). We then verified this by genescan analysis, in which the

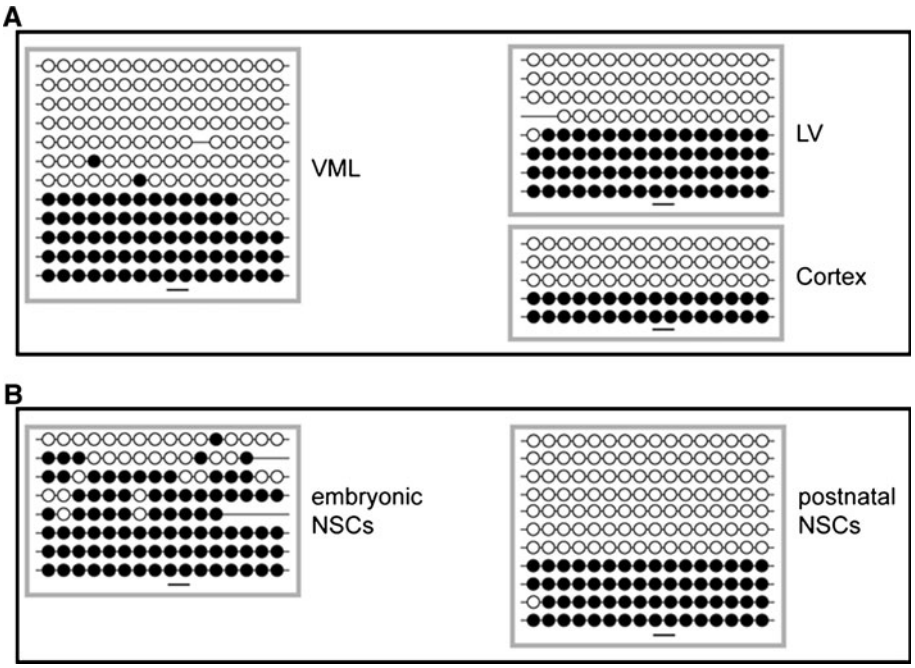

Fig. 2 Bisulfite sequencing of *SnrpN* from postnatal mouse brain tissue (**a**) and neural stem cells (NSCs, **b**). Unmethylated cytosines are represented by *open circles* and methylated cytosines are shown by *filled circles*. Each *line* represents one sequenced clone and contains 16 CpGs. CpGs undetermined in the sequencing results are not shown. The HhaI site is *underlined*. VML—ventral midline, LV—lateral ventricle

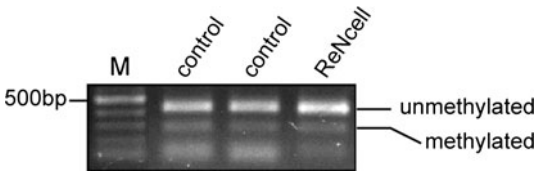

Fig. 3 Restriction digestion analysis of *SNRPN* methylation in human somatic cell and neural stem cell samples. PCR products amplified from bisulfite-treated genomic DNA was digested using HhaI. Uncut products represent the unmethylated DNA and methylation is shown by digested products. ReNcell—NSC line (ReNcell) exhibited more unmethylated products than methylated products as compared to control somatic tissue samples

amount of digested product, which represents the unmethylated form, was about half the amount that was detected in the control somatic samples (actual ratio 0.5–0.6). This indicates that the human NSC population is heterogenous, approximately 75% of alleles being unmethylated. Since the paternal allele is always unmethylated accounting for half of these, over 50% of the maternal alleles must also be unmethylated at these HhaI sites.

In order to assess to what extent this reflected a local lack of methylation at the CpGs where the Hha1 enzyme cut or more general lack of methylation of the DMR1 region, we carried out bisulfite sequence analysis of a number of clones. This revealed that a lack of digestion with Hha1 did indeed reflect lack of methylation of those sites, as expected (Fig. 5). In addition, this absence of methylation was generally associated with a large region of non-methylation of at least 8 CpGs in the region −131 to +18 in relation to the start codon of the SNRPN gene.

Methylation status of SNRPN in GCTs

The data above show that lack of methylation at the Hha1 site reflects a broader lack of methylation in the DMR1 region of the SnrpN gene in NSCs from both mice and

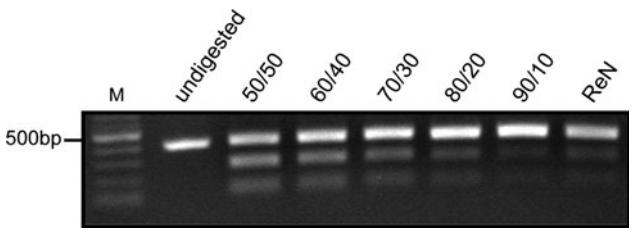

Fig. 4 Quantitation of *SNRPN* methylation in the human ReNcell NSC line. PCR products amplified from bisulfite-treated genomic DNA were digested using HhaI. Human ReN NSCs are compared to known ratios of unmethylated vs methylated controls. Quantitation using sybr-green staining revealed that in the ReNcell sample only approximately 30% of sequences cut were digested and 70% were therefore unmethylated. ReN, human ReNcell NSC line

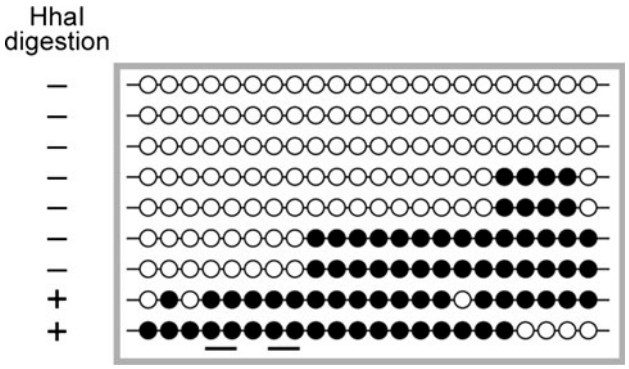

Fig. 5 Bisulfite sequencing of *SNRPN* from the ReNcell human neural stem cell line. Digestion result with Hha1 shown on left hand side and HhaI sites are *underlined*. No clones showed complete methylation of all CpGs

humans. This suggests that the same lack of methylation at the Hha1 sites in GCTs as reported by Bussey et al. [13] is also likely to reflect a lack of methylation over a broader region. However, it is also possible that it reflects more minor absence of methylation of only a few CpGs. This question can only be resolved by a more complete analysis of the methylation status in these tumours. We therefore analysed the methylation of a cohort of 20 GCTs, including 6 intracranial tumours. We first analysed a small group of these tumours by Hha1 digestion followed by Genescan to determine whether we obtained a similar result as Bussey et al. [13] (Fig. 6; Table 1). We found that five GCTs, including two intracranial germinomas, exhibited very low levels of methylation at these sites, while one (GCT 79, abdominal YST) gave a value comparable to the lowest of our control sample values.

Bisulfite sequencing showed most clones to be entirely methylated or unmethylated (data not shown). It would therefore have required a vast number of such sequences to gain statistically significant data showing if the ratio of methylation differed from the 'normal' somatic pattern of 50%. We therefore adopted an alternative strategy of bisulfite-pyrosequencing, which provides a quantitative value of the average methylation of multiple CpGs in a large number of cells. We analysed four of the CpGs of the SNRPN gene from the entire cohort of 20 tumours,

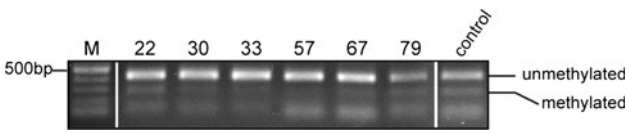

Fig. 6 Restriction digestion analysis of *SNRPN* methylation in human germ cell tumour samples. PCR products from bisulfite-treated genomic DNA were digested using HhaI. All samples showed more unmethylated products than methylated products. Control, a human somatic cell sample, numbers above show sample IDs

Table 1 Genescan analysis of *SNRPN* methylation in human GCTs. me/unme, ratio of methylated and unmethylated products

Sample	Histology	Site	Ratio (me/unme)	Relative methylation level
Controls			0.24	1
79	YST	Ovary	0.21	0.91
22	Germinoma	Testis	0.13	0.61
30	Germinoma	Brain	0.09	0.44
67	Germinoma	Brain	0.06	0.28
33	Germinoma	Ovary	0.02	0.12
57	YST	SCT	0.00	0.00

YST yolk sac tumour, *Abdo* abdomen, *SCT* sacrococcygeal, *Controls* human somatic cell samples

including two of the CpGs that had been assessed in the Hha1 digestion strategy (Table 2).

The pyrosequencing results showed that there was little variation in methylation levels between each of the four CpGs within the same sample, indicating again that the methylation status of the Hha1 sites was shared with nearby CpGs. Since this was the case, we could also therefore use the average methylation across all four CpGs as a value for comparison between samples. The value for control human genomic DNA samples provided a reference value for normal somatic imprinting. Comparison of these results to our gene scan data showed that there was a good correlation of relative values of methylation, although the pyrosequencing gave better sensitivity where the level of methylation was lowest, such as in GCT57, suggesting that pyrosequencing provides a more linear readout of methylation levels (Fig. 7).

Overall we saw a substantially reduced level of methylation in almost all GCT samples as compared to the controls (Fig. 8; Tables 3, 4), although sample 15 (an ovarian YST) was a little high even compared to controls. Amongst the other samples, there was a clear association between the absolute level of methylation and the age/type of tumour, with younger patients and YSTs exhibiting the lowest levels of methylation. However, since YSTs other than one of the cranial samples, were normally associated with the younger patients, it was not possible to disentangle this association. All six intracranial tumours exhibited very low levels of methylation.

Table 2 Pyrosequencing analysis of *SNRPN* methylation

GCT#	Histology	Site	Age(yr)	Methylation (%)			
				CpG1	CpG2*	CpG3*	CpG4
Control#1				35	38	38	37
Control#2				34	39	40	38
Control#3				32	35	34	35
Control#4				30	33	33	33
79	YST	Ovary	0	20	22	24	27
36	YST	Testis	1	12	12	12	13
38	YST	Testis	1	3	3	3	2
43	YST	Testis	1	3	2	3	3
46	YST	SCT	2	4	3	3	3
54	YST	SCT	2	14	15	16	17
57	YST	SCT	2	9	10	10	11
73	YST	Brain	3	6	6	6	6
48	YST	Abdo	9	32	32	34	34
19	YST	Ovary	9	4	3	4	4
15	YST	Ovary	12	44	51	49	52
34	YST	Brain	12	18	21	19	18
35	Germinoma	Brain	11	16	17	16	16
59	Germinoma	Ovary	12	8	8	8	13
33	Germinoma	Ovary	12	14	15	16	15
42	Germinoma	Brain	12	17	18	18	18
17	Germinoma	Ovary	14	21	23	23	23
30	Germinoma	Brain	16	16	17	17	17
67	Germinoma	Brain	17	18	21	21	20
22	Germinoma	Testis	25	29	31	32	32

The table lists the results from three independent experiments.
* CpGs that generated the HhaI site

YST yolk sac tumour, *Abdo* abdomen, *SCT* sacrococcygeal

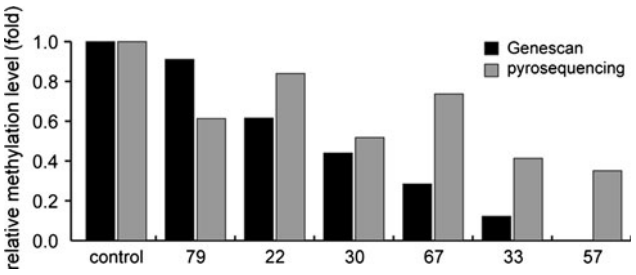

Fig. 7 Comparison of genescan and pyrosequencing results. Each *bar* represents the value of each sample relative to the controls (human somatic cells) set as 1. Genescan data is shown by *dark grey bars* and pyrosequencing results are shown by *light grey bars*. These two types of analysis produced very similar results results

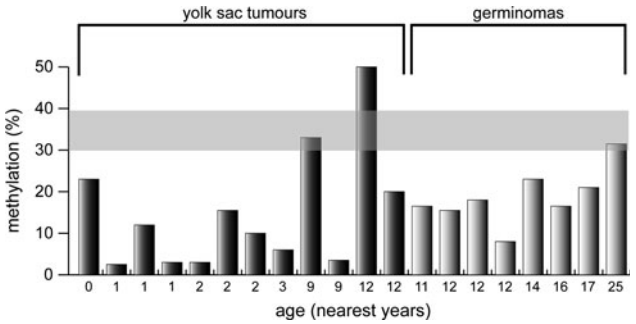

Fig. 8 Graphical representation of pyrosequencing analysis results of *SNRPN* methylation in GCTs from Table 3. *Dark grey bars* represent yolk sac tumour samples and germinoma samples are shown by *light grey bars*. The *broad grey* horizontal line shows the range of methylation levels in control somatic samples

Table 3 Pyrosequencing analysis results of *SNRPN* methylation in relation to age

Age(yr)	Methylation (%)			
	<10%	10–30%	30–40%	>40%
<4	5	3	0	0
9–18	2	7	1	1
>20	0	0	1	0

Degree of methylation grouped into those below 10% methylation and 10–30%, both of which represent different levels below the normal level of methylation seen in controls, 30–40% which is similar to controls, and >40% representing those that are more methylated than controls

Discussion

The current consensus that all GCTs, including those in the CNS, arise from PGCs is based on a number of features shared between GCTs in all locations. However, few of these features are entirely restricted to PGCs or GCTs and many do not, therefore, provide strong evidence in support of the 'germ cell origin' model. In this study we have shown that one of the strongest links between GCTs and PGCs, reduced methylation of the SNRPN gene, is also shared with some NSCs of the developing brain. Indeed, our analysis of the methylation of SNRPN in human GCTs shows that they exhibit hypomethylation rather than complete absence of methylation. Previous studies used a crude quantitation, and reported complete absence of methylation of SNRPN in some intracranial GCTs. Our detailed quantitative approaches showed no GCTs with complete absence of methylation. Also, presumably because we used a more quantitative approach, we found that the vast majority of tumour samples showed significant hypomethylation as compared to control somatic tissues, whereas Bussey et al. [13] reported only one out of five intracranial tumours exhibited a non-somatic level of methylation.

Table 4 Pyrosequencing analysis results of *SNRPN* methylation in relation to tumour type

Type	Site	Methylation (%)			
		<10%	10–30%	30–40%	>40%
YST	Gonadal	3	2	0	1
	Nongonadal	2	3	1	0
Germinoma	Gonadal	1	2	1	0
	Nongonadal	0	4	0	0

Degree of methylation grouped into those below 10% methylation and 10–30%, both of which represent different levels below the normal level of methylation seen in controls, 30–40% which is similar to controls, and >40% representing those that are more methylated than controls

YST yolk sac tumour

Hypomethylation such as we detected in GCT samples is not only seen in NSCs, as we have shown here, but also in PGCs during their migratory phase. Although erasure of imprinting in PGCs has been described as complete by E12.5, SnrpN remains significantly methylated in some cells, with as many as 10–20% of paternal alleles still completely methylated even as late as E17.5 [16, 20]. Therefore, since GCTs, PGCs and NSCs all exhibit similar levels of loss of SnrpN methylation, the degree of methylation of the SNRPN gene in human GCTs cannot reliably indicate a PGC rather than an NSC origin for these tumours.

Could NSCs provide an alternative origin for intracranial GCTs? It is true that NSCs do not normally possess the ability to form teratomas either in situ or when transplanted into permissive environment such as the kidney capsule (PJS, unpublished data). Likewise, it seems unlikely that they could form the cell types seen in germinomas. However, there is significant evidence that they might

acquire the ability to form a wide range of cell types with relative ease. NSCs can be triggered to form tissues other than neural, including haematopoietic and myogenic lineages, by disruption of DNA methylation and histone acetylation [22, 23]. Transplantation into an embryonic environment revealed an even broader potential with NSCs contributing functional cells to tissues of all three germ layers [24]. Also, when cultured in embryoid bodies alongside embryonic stem cells, NSCs could be induced to express markers of all three germ layers [25]. It is therefore clear that neural stem cells, even from adults, can adopt a broad range of cell differentiation fates if placed in an appropriate environment. More recently, it has been shown that forced expression of only one gene, Oct4, is sufficient to induce NSCs to behave as ES cells and acquire the ability to form teratomas [26, 27]. Hence, we have hypothesized that NSCs form these same cell types and therefore teratomas, if that potential is released (probably through an initial epigenetic error). Germinomas, on the other hand, would represent cells that had not acquired such a wide range of differentiation potential.

If intracranial GCTs are in fact derived from NSCs of the brain rather than misplaced PGCs, this provides a major new avenue of research to elucidate why they form, and to search for an explanation for the particular timing and position of their occurrence. Our data support an origin for GCTs from NSCs of the immature brain during embryonic and foetal development and later from NSCs restricted to the ventral midline of the brain. What is it about these cells that could make them particularly prone to form these tumours? Could an unusual methylation status of these cells mean that they are uniquely susceptible to epigenetic disruption, activating a more primitive gene expression pattern? There is indeed evidence to support such a theory. Biallelic expression of the imprinted genes, IGF2 and H19, has been demonstrated in the brains of mice [19, 28], rats [29] and humans [30]. Hemberger et al. [17] showed biallelic expression of H19 restricted to the midline structures of mice, particularly the hypothalamus and pineal regions, precisely the regions where germinomas arise in humans. They also found biallelic ventral midline expression of IGF2 even in postnatal animals. In the human CNS biallelic expression of IGF2 was again detected in the foetal brain [30].

Given the central role of Oct4 in pluripotency and in induced pluripotency of NSCs, it is important to note that Oct4 gene expression is readily activated by treatments that inhibit DNA methylation [31]. Indeed, in experiments where forced gene expression has been used to reprogramme cells, treatment with an agent to reduce gene methylation strongly enhanced these effects [32]. Hence, if cells of the CNS in particular locations (the ventral midline) or at particular times (during embryonic and fetal stages) exhibit less/more dynamic methylation, a link with increased Oct4 expression and so a more plastic behaviour seems quite feasible.

A striking feature of intracranial GCTs is that different subtypes occur at different ages, with teratomas seen predominantly prenatally and both YSTs and germinomas sharing the same peak incidence in teenagers. The 'germ cell origin' hypothesis does not provide any plausible explanation for this association between tumour type and age. With respect to our 'NSC origin' hypothesis, we suggest that the type of tumour depends upon the maturational state of the NSC when it becomes transformed. Thus, transformation of an early embryonic NSC would reveal a broad pluripotency and so teratoma formation. Transformation of a later NSC of the ventral midline in teenagers, would form the more limited cell types seen in YSTs and germinomas.

An alternative explanation for the unique timing and location of germinomas in the ventral midline of the brain in teenagers is the microenvironment of those tumours. This is a region of major hormonal activity during puberty. It may therefore be the case that tumours arise when NSCs in this region, which have acquired some defect during development, are subjected to changes in their environment that allow them to grow when they otherwise would not. This avenue of investigation would be of significant value since it might identify potential therapeutic avenues based on manipulation of the tumour microenvironment.

Acknowledgments We greatly appreciate the support of the Children's Cancer and Leukaemia Group (CCLG), especially Dr Juliet Hale and Professor Richard Grundy. VA was supported by The Samantha Dickson Brain Tumout Trust. JNJ was supported by Ali's Dream and Charlie's Challenge. RDP, JCN and NC are supported by the MRC, CRUK, CLIC Sargent, The Parthenon Trust and Addenbrooke's Charities.

References

1. Gobel U et al (2000) Germ-cell tumors in childhood and adolescence. GPOH MAKEI and the MAHO study groups. Ann Oncol 11:263–271
2. Lieuw K, Haas-Kogan D, Ablin A (2004) Intracranial germ cell tumours. In: Gupta N, Banerjee A, Haas-Kogan D (eds) Pediatric CNS tumors. Springer, Berlin, pp 107–121
3. Freeman B (2003) The active migration of germ cells in the embryos of mice and men is a myth. Reproduction 125:635–643
4. Runyan C, Gu Y, Shoemaker A, Looijenga L, Wylie C (2008) The distribution and behavior of extragonadal primordial germ cells in Bax mutant mice suggest a novel origin for sacrococcygeal germ cell tumors. Int J Dev Biol 52:333–344
5. Schneider DT et al (2001) Multipoint imprinting analysis indicates a common precursor cell for gonadal and nongonadal pediatric germ cell tumors. Cancer Res 61:7268–7276
6. Sievers S et al (2005) IGF2/H19 imprinting analysis of human germ cell tumors (GCTs) using the methylation-sensitive single-nucleotide primer extension method reflects the origin of GCTs in

different stages of primordial germ cell development. Genes Chromosomes Cancer 44:256–264
7. Rivera MN, Haber DA (2005) Wilms' tumour: connecting tumorigenesis and organ development in the kidney. Nat Rev Cancer 5:699–712
8. Zhan S, Shapiro DN, Helman LJ (1995) Loss of imprinting of IGF2 in Ewing's sarcoma. Oncogene 11:2503–2507
9. Zhan S, Shapiro DN, Helman LJ (1994) Activation of an imprinted allele of the insulin-like growth factor II gene implicated in rhabdomyosarcoma. J Clin Invest 94:445–448
10. Kondo M et al (1995) Frequent loss of imprinting of the H19 gene is often associated with its overexpression in human lung cancers. Oncogene 10:1193–1198
11. Kohda M et al (2001) Frequent loss of imprinting of IGF2 and MEST in lung adenocarcinoma. Mol Carcinog 31:184–191
12. Nishihara S et al (2000) Multipoint imprinting analysis in sporadic colorectal cancers with and without microsatellite instability. Int J Oncol 17:317–322
13. Bussey KJ et al (2001) SNRPN methylation patterns in germ cell tumors as a reflection of primordial germ cell development. Genes Chromosomes Cancer 32:342–352
14. Oosterhuis JW, Stoop H, Honecker F, Looijenga LH (2007) Why human extragonadal germ cell tumours occur in the midline of the body: old concepts, new perspectives. Int J Androl 30:256–263 discussion 263–264
15. Scotting PJ (2006) Are cranial germ cell tumours really tumours of germ cells? Neuropathol Appl Neurobiol 32: 569–574
16. Li JY, Lees-Murdock DJ, Xu GL, Walsh CP (2004) Timing of establishment of paternal methylation imprints in the mouse. Genomics 84:952–960
17. Rugg-Gunn PJ, Ferguson-Smith AC, Pedersen RA (2005) Epigenetic status of human embryonic stem cells. Nat Genet 37:585–587
18. White HE, Durston VJ, Harvey JF, Cross NCP (2006) Quantitative analysis of SRNPN gene methylation by pyrosequencing as a diagnostic test for Prader–Willi syndrome and angelman syndrome. Clin Chem 52:1005–1013
19. Hemberger M et al (1998) H19 and Igf2 are expressed and differentially imprinted in neuroectoderm-derived cells in the mouse brain. Dev Genes Evol 208:393–402
20. Hajkova P et al (2002) Epigenetic reprogramming in mouse primordial germ cells. Mech Dev 117:15–23
21. Donato R et al (2007) Differential development of neuronal physiological responsiveness in two human neural stem cell lines. BMC Neurosci 8:36
22. Schmittwolf C et al (2005) In vivo haematopoietic activity is induced in neurosphere cells by chromatin-modifying agents. EMBO J 24:554–566
23. Galli R et al (2000) Skeletal myogenic potential of human and mouse neural stem cells. Nat Neurosci 3:986–991
24. Clarke DL et al (2000) Generalized potential of adult neural stem cells. Science 288:1660–1663
25. Denham M et al (2006) Neural stem cells express non-neural markers during embryoid body coculture. Stem Cells 24: 918–927
26. Kim JB et al (2009) Oct4-induced pluripotency in adult neural stem cells. Cell 136:411–419
27. Kim JB et al (2009) Direct reprogramming of human neural stem cells by OCT4. Nature 461:649–653
28. Hu JF, Vu TH, Hoffman AR (1995) Differential biallelic activation of 3 Iinsulin-like growth factor-II promoters in the mouse central nervous system. Mol Endocrinol 9:628–636
29. Pedone PV et al (1994) Parental imprinting of rat insulin-like growth factor-II gene promoters is coordinately regulated. J Biol Chem 269:23970–23975
30. Pham NV, Nguyen MT, Hu JF, Vu TH, Hoffman AR (1998) Dissociation of IGF2 and H19 imprinting in human brain. Brain Res 810:1–8
31. Ruau D et al (2008) Pluripotency associated genes are reactivated by chromatin-modifying agents in neurosphere cells. Stem Cells 26:920–926
32. Mikkelsen TS et al (2008) Dissecting direct reprogramming through integrative genomic analysis. Nature 454:49–55